

Article

Concentrations and Fractionation of Carbon, Iron, Sulfur, Nitrogen and Phosphorus in Mangrove Sediments Along an Intertidal Gradient (Semi-Arid Climate, New Caledonia)

Jonathan Deborde ¹, Cyril Marchand ^{1,*}, Nathalie Molnar ^{1,2}, Luc Della Patrona ³
and Tarik Meziane ²

¹ Institut de Recherche pour le Développement (IRD), UR 206, UMR 7590—IMPMC, F-98848 New Caledonia, France; E-Mails: jonathan.deborde@gmail.com (J.D.); nathaliemolnar@gmail.com (N.M.)

² UMR BOREA 7208 CNRS-MNHN-UPMC-IRD-UCBN, Muséum National Histoire Naturelle, CP 53, 61 rue Buffon, 75231 Paris cedex 05, France; E-Mail: meziane@mnhn.fr

³ Département Lagons, Ecosystèmes et Aquaculture Durable (LEAD/NC), Ifremer, 101, Promenade Roger Laroque, Center IRD, BP 2059–98846 Nouméa Cedex, Nouvelle-Calédonie; E-Mail: Luc.Della.Patrona@ifremer.fr

* Author to whom correspondence should be addressed; E-Mail: cyril.marchand@ird.fr; Tel.: +33637081531.

Academic Editors: Joseph M. Smoak and Christian Joshua Sanders

Received: 2 November 2014 / Accepted: 4 February 2015 / Published: 10 February 2015

Abstract: In mangrove ecosystems, strong reciprocal interactions exist between plant and substrate. Under semi-arid climate, *Rhizophora* spp. are usually predominant, colonizing the seashore, and *Avicennia marina* develops at the edge of salt-flats, which is the highest zone in the intertidal range. Along this zonation, distribution and speciation of C, Fe, S, N, and P in sediments and pore-waters were investigated. From the land-side to the sea-side of the mangrove, sediments were characterized by I/ increase in: (i) water content; (ii) TOC; (iii) mangrove-derived OM; II/ and decrease in: (i) salinity; (ii) redox; (iii) pH; (iv) solid Fe and solid P. Beneath *Avicennia* and *Rhizophora*, TS accumulated at depth, probably as a result of reduction of iron oxides and sulfate. The loss of total Fe observed towards the sea-side may be related to sulfur oxidation and to more intense tidal flushing of dissolved components. Except the organic forms, dissolved N and P concentrations were very low

beneath *Avicennia* and *Rhizophora* stands, probably as a result of their uptake by the root systems. However, in the unvegetated salt-flat, NH_4^+ can accumulate in organic rich and anoxic layers. This study shows: (i) the evolution of mangrove sediment biogeochemistry along the intertidal zone as a result of the different duration of tidal inundation and organic enrichment; and (ii) the strong links between the distribution and speciation of the different elements.

Keywords: mangrove; zonation; biogeochemistry; New Caledonia

1. Introduction

Mangroves are the dominant ecosystems of tropical and subtropical coastlines, covering nearly 140,000 km² [1]. Beyond their ecological, sociological, and economical roles [2–4], mangroves are of great interest for the study of biogeochemical cycles, notably because of marine and fresh water mixing, and because large amount of carbon accumulation [5,6]. Pathways of organic matter decomposition in mangrove sediments are diverse, from aerobic respiration to anaerobic sulfate reduction, through denitrification, manganese respiration and iron respiration, leading to a high variability of elements distribution and speciation [7]. In addition to the quality and the quantity of organic inputs, sedimentation rates, and biological activities, other parameters have to be taken into account to understand mangrove sediments biogeochemistry, e.g., the tree species and their age, tides and bioturbation [8–11]. Additionally, strong interactions between mangrove plants and substrate geochemistry were demonstrated, resulting in the zonation of the ecosystem [12–14]. Extension, secretion and absorption of nutrients by the root system, as well as the oxygenation capacity of the soil, are characteristic of each plant species [10,15]. Consequently, concentration and fractionation of major elements may depend on mangrove stands. In New-Caledonia, mangrove forests are developed over 35,000 ha, fringing on about 80% and 15% of the western and the eastern coastline of the island, respectively [16]. Previous studies [17,18] suggested that the main factor controlling the distribution of mangrove species in New Caledonia was soil salinity, which in turn was controlled by the duration of tidal inundation and thus by the soil elevation [19]. Thus, our hypothesis are that towards the sea-side: (i) the sediment will be enriched in organic matter because of higher productivity resulting from less stressing conditions; (ii) the sediments will be more reducing because of longer waterlogging and higher organic content; (iii) and the concentrations of key nutrients will be lower because of plant uptake. The main objective of the present study was to understand how the distribution of the different mangrove vegetation along the intertidal zone may influence the distribution and the speciation of C, N, P, Fe, and S in mangrove sediments and pore-waters.

2. Material and methods

2.1. Study Site

Mangroves in New Caledonia are dominated by *Rhizophora* spp. (55% of the total mangrove area), and *Avicennia marina* (14%). Salt-flat represents 26% of the total mangrove area. The study was conducted in a fringing mangrove located in Saint Vincent Bay, New Caledonia (Figure 1). This mangrove

(21°54' S, 166°04' E), covering 20 ha, does not receive any significant freshwater runoff, and was free of anthropogenic influences. This forest exhibits the typical zonation of mangroves in New Caledonia [18]: (i) at the back side of the mangrove swamp, the area is occupied by the salt-flat, a highly saline zone, only submerged during high spring tide and covered sporadically in the most downstream stretches with bushes of *Sarcocornia quinqueflora*; (ii) a second stand of vegetation, downstream, is occupied by *Avicennia marina*; (iii) finally, the seaward edge is occupied by *Rhizophora stylosa*, which is submerged at each tide. Tides are semidiurnal, and mangroves were fully drained at each low tide, except during neap tides where parts of the *Rhizophora* area remain flooded. The landward *Avicennia* was sparsely distributed, bush-like and never exceeded 1 m in height. The seaward *Rhizophora* zone had a relatively low density and individual trees rarely exceeded 3 m in height. Fiddler crabs, *Uca* spp., were present in the salt-flat and *Avicennia* stands with high density of burrows. Density was estimated using photography of sampling sites, and was about 20 and 30 burrows·m⁻² for the salt-flat and *Avicennia*, respectively. In the *Rhizophora* forest, the main crab specie present was a *Grapsidae* with an estimate density of about 40 burrows·m⁻². Three sampling sites were chosen corresponding to the three vegetation stands (Figure 1).

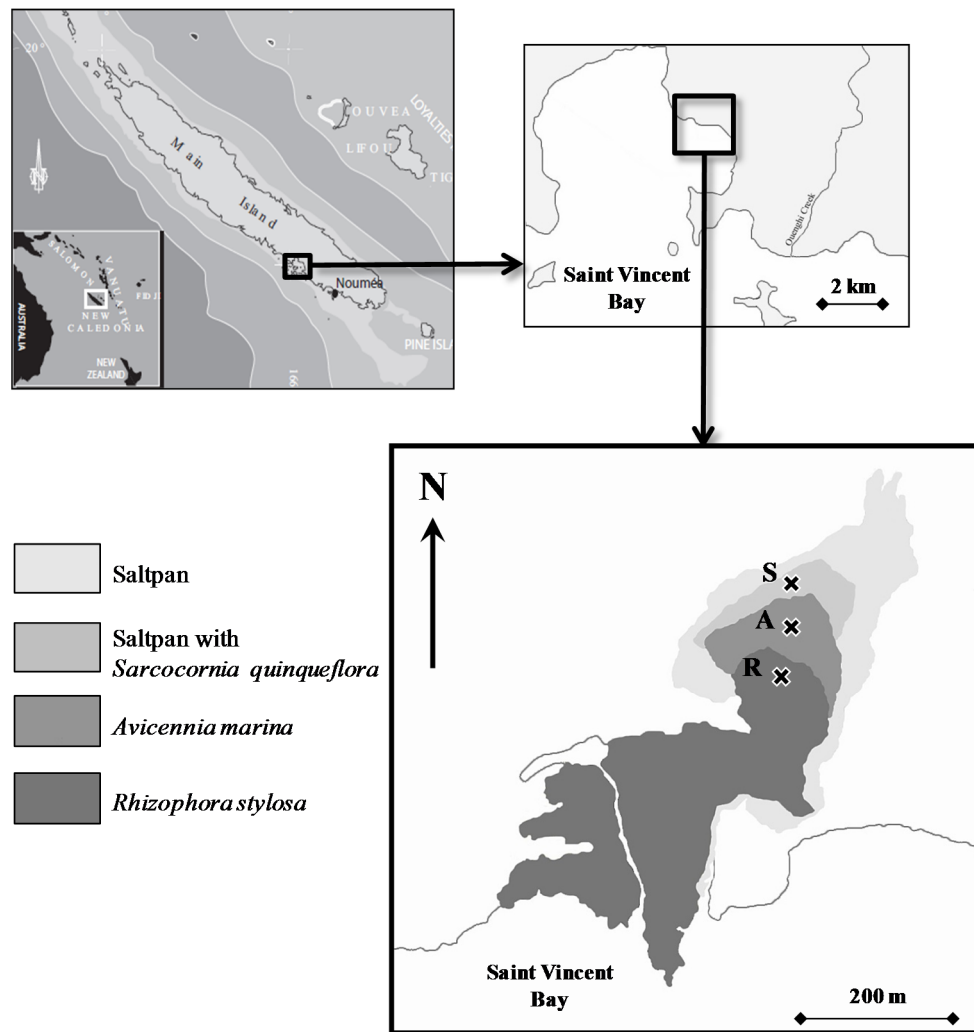


Figure 1. Map showing the location of the studied mangrove in Saint Vincent Bay on the west coast of New Caledonia, with vegetation zonation and the location of sampling sites in: (S) Salt-flat with *Sarcocornia quinqueflora*, (A) *Avicennia marina* and (R) *Rhizophora stylosa*.

2.2. Sampling Collection

Sediment cores (50 cm) were collected in June 2009. Considering the low tidal range in New Caledonia, this sampling depth allowed us to reach the redox boundary between the unsaturated zones (evolving with tides) and the saturated zone. In addition, we were interested in the possible role of the root system; the latter mainly develop in the upper 50 cm considering the limited development of trees in this semi-arid climate. Cores were sampled in triplicate during low tide using an Eijkelkamp gouge auger in each mangrove stand. Core locations were chosen close to the vegetation but carefully avoiding the presence of main roots in samples. After being collected, cores were wrapped in plastic film and aluminum foil to prevent oxidation and photo-oxidation, and were transported to an air conditioned laboratory within 10 min. Samples were collected every 5 cm from 0 to 50 cm depth. Sediment sub-samples were taken and immediately sealed in a pre-weighed vial, and frozen for analyses of Fe and P solid fractions, and water content determination. A second sediment sub-sample was taken and was freeze-dried for analyses of total organic carbon (TOC), organic matter characterization (stable isotope composition: $\delta^{13}\text{C}$ and $\delta^{15}\text{N}$) and total sulfur (TS). Pore-waters were collected using soil moisture samplers Rhizon[®] (Eijkelkamp Agrisearch Equipment, Giesbeek, The Netherlands) [20,21]. This method allowed us to extract 20 mL from 5 cm long sediment section. After filtration through 45 μm cellulose acetate syringe-filter, one aliquot was acidified with HNO_3 and store refrigerated for Fe analysis (Fe^{2+} and Fe^{3+}), a second was frozen at $-25\text{ }^\circ\text{C}$ for nutrient analysis (NH_4^+ , NO_x , DON; DIP, DOP).

2.3. Analytical Methods

2.3.1. Salinity, pH, Redox Potential and $\Sigma\text{H}_2\text{S}$ Measurements

Salinity, pH, redox and $\Sigma\text{H}_2\text{S}$ were measured in an air-conditioned laboratory within 30 min after the core sampling [17]. pH and redox were measured using a WTW pH/mV/T meter. Redox data are reported relative to a standard hydrogen electrode after adding 202 mV to the original mV values obtained with an Ag/AgCl reference electrode at $25\text{ }^\circ\text{C}$. A Wilcoxon–Mann–Whitney (WMW) test was used to compare mean values for pairs (Salt-flat vs. vegetated zone, *Rhizophora* vs. *Avicennia*). An Atago manual refractometer was used to determine salinity from pore-water extracted with Rhizon. The determination of the total sulfide concentration (TS, S^{2-} , H_2S and HS^- , [22]) was done with a WTW sulfide ion specific electrode ($(\log(\text{S}^{2-}) = -0.024 \times E(\text{V}) - 0.878)$, [10]).

2.3.2. Pore-Water Analysis

Dissolved iron (Fe^{2+} and Fe^{3+}) were determined by colorimetric procedures with a precision of $\pm 5\%$ [23,24]. A nephelometric method adapted from [25] was used to determine sulfate (with a precision of about 5%). NH_4^+ concentrations were measured with a TD700 fluorimeter (TurnerDesigns, Sunnyvale, CA, USA) following the method of Holmes *et al.* [26]. The method of Bendschneider and Robinson (1952, [27]) was used to determine NO_x (nitrate + nitrite) concentrations, using an Autoanalyzer III (Bran+Luebbe, Norderstedt Germany). Dissolved inorganic phosphorus (DIP) concentrations were determined using the autoanalyzer III (Bran+Luebbe, Norderstedt, Germany) [28]. Following a persulfate wet-oxidation in low alkaline condition, total dissolved nitrogen (TDN) and

phosphorus (TDP) concentrations were determined as NO_x and DIP according to the method of Raimbault (1999, [29]). Dissolved organic fractions (DON and DOP) concentrations were calculated by difference between the measured TDN and TDP and the measured inorganic nitrogen (NH_4^+ and NO_x) and phosphorus (DIP).

2.3.3. Sediment Solid Phase Analysis

2.3.3.1. Total Organic Carbon, Total Sulfur

Total organic carbon (TOC), hydrogen index (HI) and oxygen index (OI), were determined using a Rock-Eval 6 pyrolysis [30,31]. Briefly, samples are first pyrolysed under an inert N_2 atmosphere and the residual carbon is subsequently burnt in an oxidation oven. The amount of hydrocarbons (HC) released during pyrolysis is detected with a flame ionization detector (FID) (Vinci Technology, Nanterre, France), while online infrared detectors measure continuously the released CO and CO_2 . Classical Rock-Eval parameters are calculated by integration of the amounts of HC, CO and CO_2 produced during thermal cracking of the OM, between well-defined temperature limits. HI corresponds to the quantity of HC released relative to TOC (in $\text{mg}\cdot\text{HC}\cdot\text{g}^{-1}\cdot\text{TOC}$) and correlating with the H/C ratio. OI corresponds to the quantity of oxygen released as CO and CO_2 during pyrolysis, relative to TOC (in $\text{mg}\cdot\text{HC}\cdot\text{g}^{-1}\cdot\text{TOC}$) and correlating with the O/C ratio. A CNS-2000 LECO apparatus was used to determine total nitrogen and total sulfur (TS) concentrations (combustion at 1100 °C).

2.3.3.2. Stable Isotope Analysis

Sediment samples for stable-isotope analysis ($\delta^{13}\text{C}$ and $\delta^{15}\text{N}$) were freeze-dried before being ground with a mortar. Analysis were made with a PDZ Europa ANCA-GSL elemental analyzer (Sercon Ltd., Cheshire, UK) interfaced to a PDZ Europa 20–20 isotope ratio mass spectrometer (Sercon Ltd., Cheshire, UK) at the UC Davis Stable Isotope Facility laboratory. After sample combustion at 1000 °C in a reactor packed with chromium oxide and silvered cobaltous/cobaltic oxide, oxides were removed in a reduction reactor (reduced copper at 650 °C). Then, helium carrier flows through a water trap (magnesium perchlorate) and an optional CO_2 trap (for N-only analyses). Eventually, N_2 and CO_2 were separated on a Carbosieve GC column (65 °C, $65\text{ mL}\cdot\text{min}^{-1}$) before entering the IRMS.

2.3.3.3. Particulate Iron and Phosphorus Extractions

The water content of sediments was determined by weight loss after freeze-drying, sea salt correction was applied. Particulate iron and phosphorus extractions were conducted like previously described in Deborde *et al.* [32]. An ascorbate reagent was added to the dried solid sample to remove the most reactive Fe (III) phases (Fe_{ASC}) and the associated phosphorus (P_{ASC}) from the sediment [33,34]. Acid-soluble iron (Fe_{HCl}) and phosphorus (P_{HCl}) extraction was carried out with 1M HCl, which dissolves amorphous Fe oxides, FeS, Fe phyllosilicates and carbonates [34]. P_{HCl} originated from detrital and authigenic phosphate minerals, as well as carbonates [34,35]. For both extractions, about 100 mg of dry sample was leached with 10 mL of solution. Solutions were shaken continuously during 24 h at room temperature. Samples were centrifuged after extraction, and Fe and P contents of the supernatant were determined

spectrophotometrically using the ferrozine and molybdate methods. Blank solutions experienced the same treatment. The precision estimated from replicates was $\pm 5\%$ for P and $\pm 7\%$ for Fe.

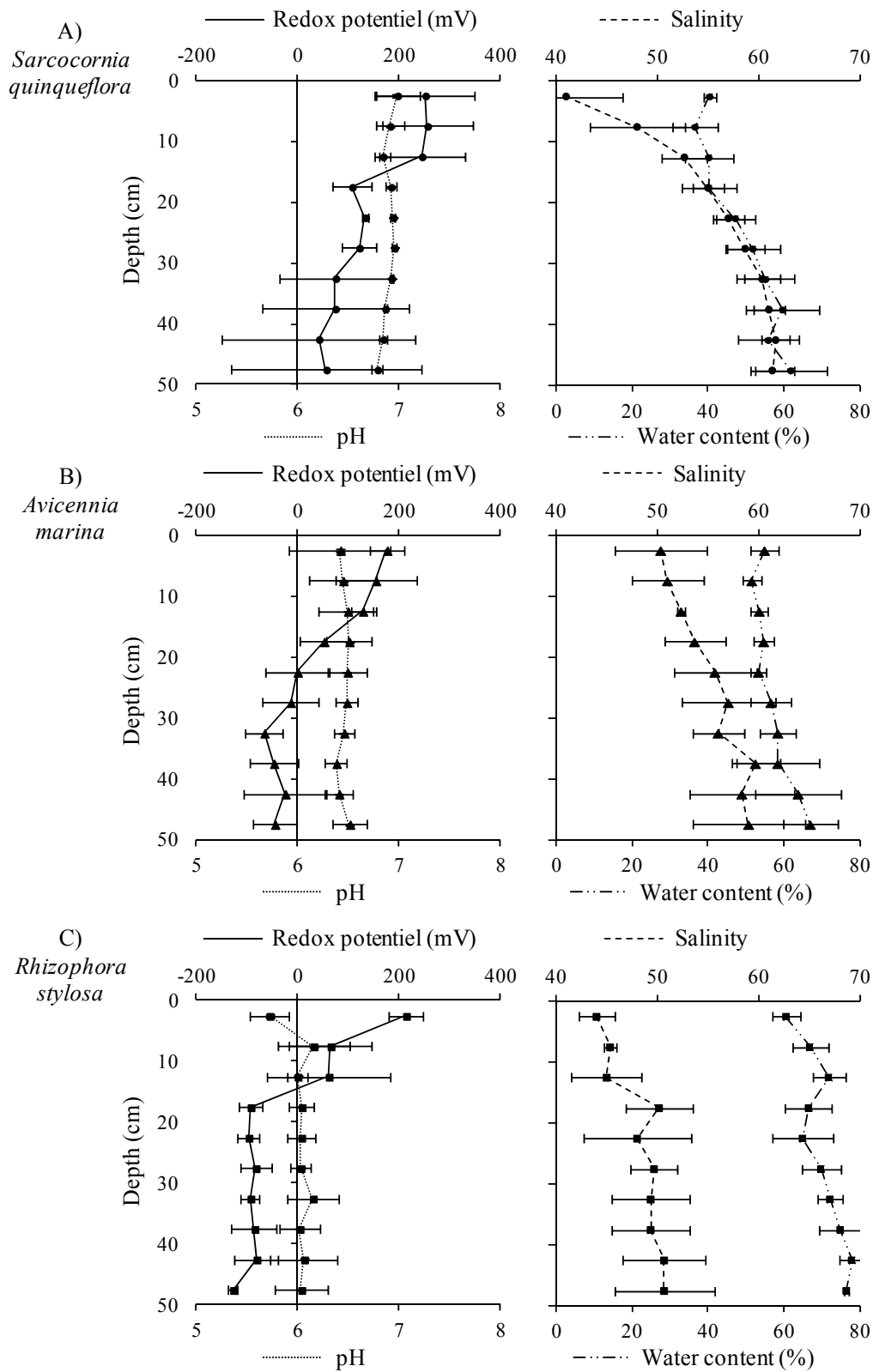


Figure 2. Mean values ($n = 3$) and standard deviation of redox potential, pH, salinity and water content measured in the sediment from surface to 50 cm depth of the three mangrove vegetation stands.

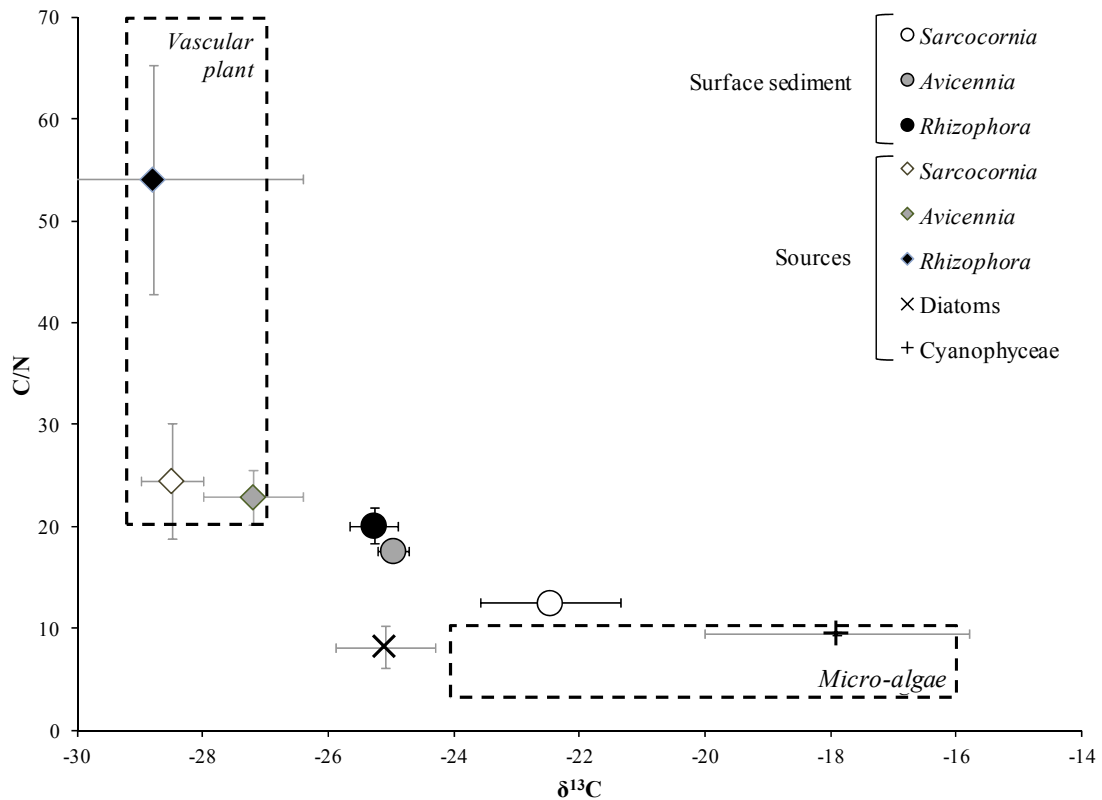


Figure 3. Mean C/N and δ¹³C values of surface sediment for each mangrove stand, and values of organic matter source identified in the mangrove. The range of values typically encountered in the literature for vascular mangrove plants (Bouillon *et al.*, 2003, Marchand *et al.*, 2005) and micro-algae (Meyers, 1994) were indicated by the dotted rectangles.

3. Results and Discussion

3.1. Influence of Mangrove Zonation on Sediment Physico-Chemical Properties and Organic Matter Content

From the salt-flat to the *Rhizophora* stand, sediment water content increased, with mean values of 49% ± 2% and 71% ± 3%, respectively, while mean salinity value decreased, from 55 to 42 (Figure 2a–c). In addition, both parameters increased with depth in every stands, particularly in the salt-flat area, where salinity reached more than 60. This depth increase may result from convection processes leading to high and stable salinity along the year as suggested by Marchand *et al.* [10]. The water content and salinity gradients most likely resulted from differences in tidal inundation between stands, which is the main factor controlling mangrove zonation in New Caledonia [17,19]. Pore-water salinity decreased towards the *Rhizophora* stand, where evaporation processes are limited due to the rare periods of emersions. Mangrove plants have different abilities to cope with pore-water salinity, *Avicennia* trees are better adapted to high salinities than *Rhizophora* trees, explaining thus its higher tidal position. However, the energy cost of this adaptation limits the tree development of *Avicennia*, which only form dwarf stands in New Caledonia. Consequently, we suggest that such a zonation and adaptation may also have an influence on mangrove productivity and thus on organic carbon accumulation in the sediment. C/N

and $\delta^{13}\text{C}$ values of the main organic matter sources are displayed in Figure 3. C/N and $\delta^{13}\text{C}$ values were 24.5 ± 5.6 and $-28.5\text{‰} \pm 0.5\text{‰}$ for *Salicornia*, 22.9 ± 2.7 and $-27.2\text{‰} \pm 0.8\text{‰}$ for *Avicennia*, 54.1 ± 11.3 and $-28.8\text{‰} \pm 2.4\text{‰}$ for *Rhizophora*, respectively. C/N values measured for diatoms and cyanophyceae were 8.2 ± 2.1 and 9.5 ± 0.2 , respectively, and their $\delta^{13}\text{C}$ values were $-25.1\text{‰} \pm 0.8\text{‰}$ and $-17.9\text{‰} \pm 2.1\text{‰}$, respectively. C/N and $\delta^{13}\text{C}$ values of the leaves of the two studied mangrove species and *Salicornia* are consistent with those found in the literature [36,37]. TOC, C/S, HI and OI measured in sediment cores of the different stands are displayed in Figure 4. In the upper sediment, TOC increased from the salt-flat (2%) to the *Rhizophora* stand (19%). Mangrove TOC values usually range between 0.5% and 15%, with a median TOC around 2.2% [7]. The sedimentary organic matter has C/N and $\delta^{13}\text{C}$ values ranging between those of the leaves and those of micro-algae (Figure 3). Mean $\delta^{13}\text{C}$ value in salt-flat sediments was $-22.5\text{‰} \pm 1.1\text{‰}$, and was lower beneath *Avicennia* and *Rhizophora*: $-25\text{‰} \pm 0.2\text{‰}$ and $-25.3\text{‰} \pm 0.4\text{‰}$, respectively (Figure 3). C/N values increased from the land-side to the sea-side of the mangrove: 12.5 ± 0.6 beneath *Sarcocornia*, 17.6 ± 0.6 beneath *Avicennia*, and 20.1 ± 1.7 beneath *Rhizophora* (Figure 3). Consequently, the contribution on mangrove-derived OM to the sedimentary organic pool increased towards the seaside. Due to its low intertidal position, the *Rhizophora* zone receives more nutrients, which favor both tree development and organic accumulation in sediments. In addition to leaf litter and micro-algae, a strong input of OM derived from root systems was evidenced with the increase of HI values from surface to mid-depth from 150 to 220, and from 200 to 250 $\text{mg}\cdot\text{HC}\cdot\text{g}^{-1}\cdot\text{TOC}$ beneath the *Avicennia* and the *Rhizophora* stands respectively. Fresh mangrove tissues are characterized by HI values ranging from 400 to 600 $\text{mg}\cdot\text{HC}\cdot\text{g}^{-1}\cdot\text{TOC}$, and OI values ranging from 100 to 200 $\text{mg}\cdot\text{O}_2\cdot\text{g}^{-1}\cdot\text{TOC}$ [30]. OM decomposition induces its dehydrogenation and oxidation, and thus a decrease of HI values and an increase of OI values. In the present study, HI values ranged between 60 and 230 $\text{mg}\cdot\text{HC}\cdot\text{g}^{-1}\cdot\text{TOC}$, evidencing that even in the upper sediment, OM was already well decomposed. Higher OI values in the upper layer than at depth may be related to the redox conditions. In fact, the deeper layers were strongly anoxic and C/S ratios close to 2, showing intense sulfuration processes, and thus, probably less efficient oxidation. Eventually, below 30 cm depth of three studied stands, sediments presented an organic carbon rich layer (8% to 16%), characterized by higher C/N ratios (29.9 to 41.7) and lower $\delta^{13}\text{C}$ and $\delta^{15}\text{N}$ values, below -25.2 and 1.8 respectively (Table 1), typical of higher plant debris. These layers were visually enriched with red *Rhizophora* tissues. This organic-rich sediments may be related to a sudden change in sea level coupled with a massive sedimentary deposit that had buried a former mangrove as previously reported in New Caledonia [18] or in Guadeloupe mangroves [38]. To summarize, in the upper layers from the land-side to the sea-side of the mangrove, the sediment was characterized by gradients in water content, salinity, TOC, and mangrove derived-OM. The gradients above are also associated with redox and pH values. Redox values decreased from the land-side to the sea-side, and with depth. Within the salt-flat, redox potential was high and stable in the upper 10 cm, with a maximum value of 255 ± 29 mV that decreased to 60 mV at depth (Figure 2a). Sediments of *Avicennia* and *Rhizophora* had significantly lower redox potentials for all depths than the salt-flat (WMW test, $p < 0.05$), while difference was not significant between *Avicennia* and *Rhizophora* sediments (WMW test, $p > 0.05$). Beneath *Rhizophora*, redox values decreased rapidly with depth, from 213.9 ± 13 to -92 ± 18 mV. Salt-flat sediments presented the less reducing conditions of the three vegetation stands because of the short tidal inundation associated with desiccation mud cracks that allowed inflow of atmospheric oxygen, and of the presence of crab burrows, which can promote oxygen

penetration ([39,40], Figure 2). The higher OM concentrations in *Avicennia* sediments led to lower redox values compare to salt-flat (Figure 2). Nevertheless, suboxic conditions (high redox potential and presence of dissolved iron) remained in the upper 15 cm. These suboxic conditions were favored by the high oxygenation capacity of the radial cable roots of *Avicennia* [10,12,41], and *Uca* sp. activity, which were also present in this stand. Within the *Rhizophora* stand, redox condition became rapidly anoxic with depth due to the high OM content, the high water content, and the low oxygenation capacity of *Rhizophora* roots [10,41]. Eventually, there was also a gradient of pH values from the land-side to the sea-side of the mangrove, 6.9 ± 0.1 in the *Sarcocornia* stand (Figure 2a), 6.5 ± 0.1 beneath *Avicennia* (Figure 2b), and 6.0 ± 0.1 in the *Rhizophora* stand (Figure 2c). Acidity of mangrove sediments can derive from organic matter decomposition, TOC concentrations increasing towards the sea, and/or sulfide oxidation (see next chapter).

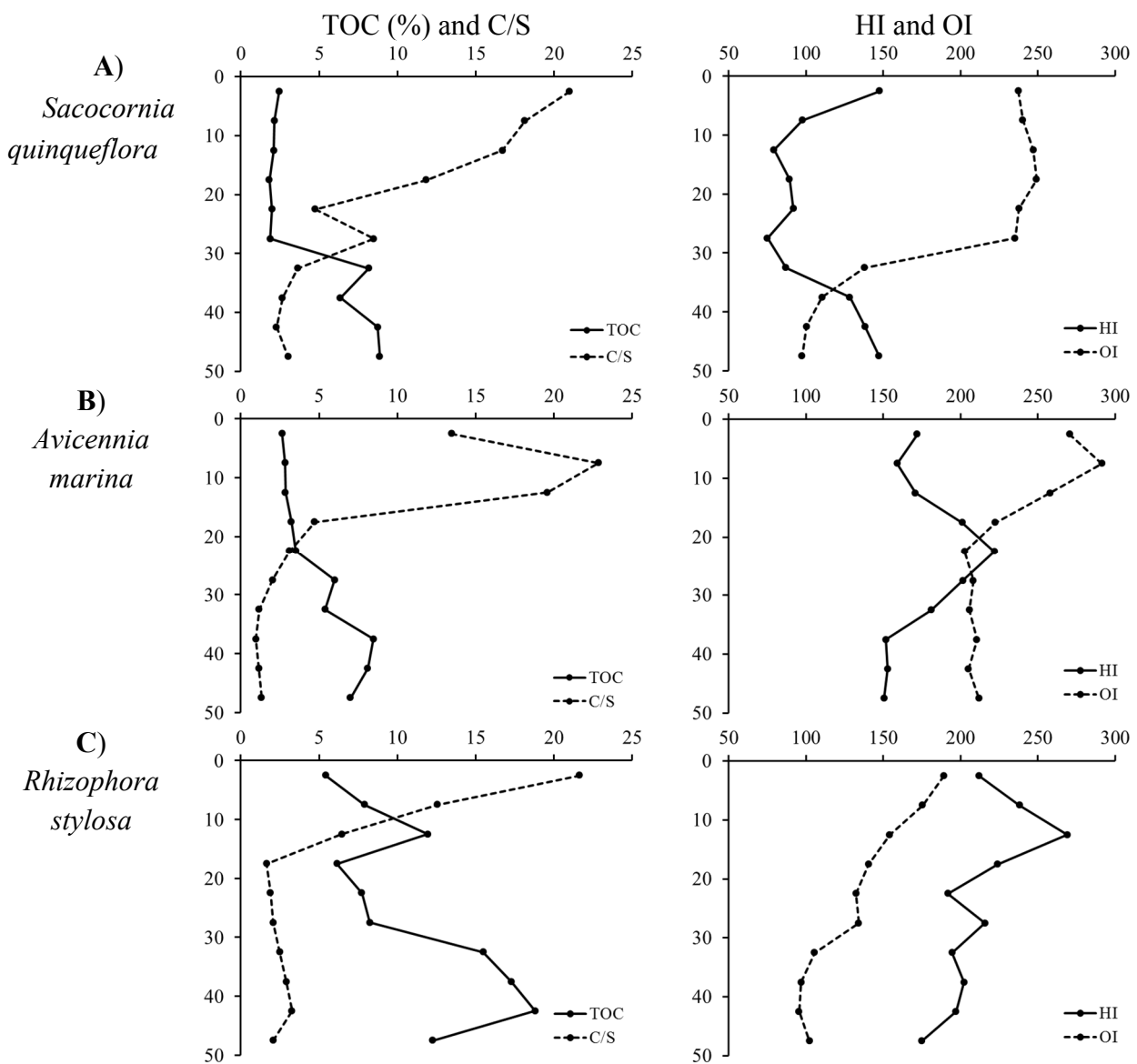


Figure 4. Total Organic Carbon (TOC%), Hydrogen Index (HI), C/S Ratios and Oxygen Index (OI) values in sediments of the three vegetation stands.

Table 1. Mean C/N ratios, $\delta^{13}\text{C}$ and $\delta^{15}\text{N}$ values of sediments in *Avicennia marina* stand. Standard deviations are indicated in italics. (Isotopic data were not available for sediments collected beneath the salt-flat and the *Rhizophora* stand).

Depth (cm)	C/N		$\delta^{13}\text{C}$		$\delta^{15}\text{N}$	
		<i>SD</i>		<i>SD</i>		<i>SD</i>
0–5	12.4	<i>1.5</i>	–23.3	<i>1.1</i>	2.8	<i>0.8</i>
5–10	14.7	<i>1.1</i>	–24.1	<i>0.2</i>	2.3	<i>0.1</i>
15–20	16.4	<i>2.1</i>	–23.9	<i>0.2</i>	2.0	<i>0.5</i>
30–35	29.9	<i>8.8</i>	–25.2	<i>1.1</i>	1.8	<i>0.4</i>
40–45	41.7	<i>12.5</i>	–26.1	<i>0.6</i>	1.7	<i>0.2</i>

3.2. Distribution and Speciation of Redox Sensitive Elements: Iron and Sulfur

Total iron ($\text{Fe}_{\text{ASC}} + \text{Fe}_{\text{HCl}}$) decreased from the salt-flat to the *Rhizophora* stand. In the sediments of the *Avicennia* and *Rhizophora* stands, Fe_{ASC} and Fe_{HCl} concentrations showed the same trend: decreasing from the top to mid-depth, and then slightly increasing, especially in the ascorbate fraction below 30 cm deep. Total iron concentrations in sediments of the salt-flat were very high in the upper 30 cm reaching $123 \pm 106 \mu\text{mol}\cdot\text{g}^{-1}$ for Fe_{ASC} and $232 \pm 83 \mu\text{mol}\cdot\text{g}^{-1}$ for Fe_{HCl} (Figure 5a). In New Caledonia, mangroves act as a barrier between the largest lagoon in the world and lateritic soils exploited for their richness in trace metals, mainly Ni and Cr. Lateritic soils are primarily composed of Fe(III)-bearing goethite and phyllosilicates [42]. The mangrove studied here does not develop downstream an ultramafic watershed. However, due to coastal current [43], some of these minerals may have been deposited in the mangrove, explaining the high concentrations of Fe measured in the solid phase. Within the salt-flat, reduced dissolved iron (Fe^{2+}) was very low ($<8 \mu\text{mol}\cdot\text{L}^{-1}$) on the whole depth profile, while in *Avicennia* and *Rhizophora* sediments, concentrations were maximum in the upper 20 cm, up to $100.0 \mu\text{mol}\cdot\text{L}^{-1}$, and decreased with depth (Figure 5). In the upper layers of the *Avicennia* and *Rhizophora* stands, the presence of Fe^{3+} , Fe^{2+} and reactive solid iron (Fe_{ASC}) reflects the reduction of iron oxides during OM decay processes. The absence of Fe^{3+} and the very low Fe^{2+} concentrations in the oxic upper layer of the salt-flat may indicate that iron oxide reduction did not occur in these sediments, or that as soon as it produced, Fe^{3+} precipitated as ferrihydrite and lepidocrocite [44]. Presence of Fe(III) has an influence on sulfur cycling in sediments because it is involved in the oxidation of reduced free sulfide, sulphato-reduction being the main process of OM decomposition in mangroves [45,46]. In the three vegetation stands, there is a significant increase in total particulate sulfur below the upper suboxic zone, up to 10% beneath *Avicennia*, while free sulfides were only detected in *Rhizophora* sediments, reaching a maximum value of $3.4 \pm 3.5 \mu\text{mol}\cdot\text{L}^{-1}$ (Figure 5). Concentrations in free dissolved sulfides ($\text{H}_2\text{S} + \text{HS}^- + \text{S}^{2-}$) are usually low in mangrove environment because they are rapidly precipitated as pyrite in presence of dissolved iron [34]. In mangroves, TS is mainly composed of pyrite whose synthesis and stabilization are favored in the most reduced sediment horizons [11]. Noel *et al.*[44] showed that goethite, the major Fe hosts in the upward horizons of a mangrove developing downstream lateritic soils, progressively disappears with increasing depth, where Fe(II)-bearing pyrite forms, as a result of a sulfate-reduction process. In addition to reduction, intense re-oxidation of aqueous Fe(II) and Fe-sulfides are suspected, and can lead to the high dissolved iron concentrations as well as to the low measured pH.

Such process was detected by Noel *et al.* [44], which results in the formation of ferrihydrite, lepidocrocite and likely goethite in *Avicennia* and *Rhizophora* sediments. In addition, these authors found that the relative proportion of a newly formed and poorly ordered iron-oxyhydroxides was higher in the *Rhizophora* mangrove stand, suggesting that tidal fluctuations may lead to uninterrupted Fe reduction-oxidation cycles. The closer is the stand to the shore, the more intense are Fe reduction-oxidation cycles. In addition, concentrations of solid Fe phases (Fe_{ASC} and Fe_{HCl}) decreased from the land-side to the sea-side of the mangrove in this study, confirming Noel *et al.* [44] hypothesis of a Fe loss from the salt-flat to the *Rhizophora* stand (*i.e.*, from the land to the shore). The loss of Fe with tides may also explain why dissolved sulfides were only detected in *Rhizophora* sediments. Those sediments are the richest in organic matter, are not limited in sulfate due to the sea proximity and are characterized by intense sulfide precipitation and dissolution. However dissolved Fe might be exported, and the remaining amount cannot compensate for the production of free dissolved sulfides.

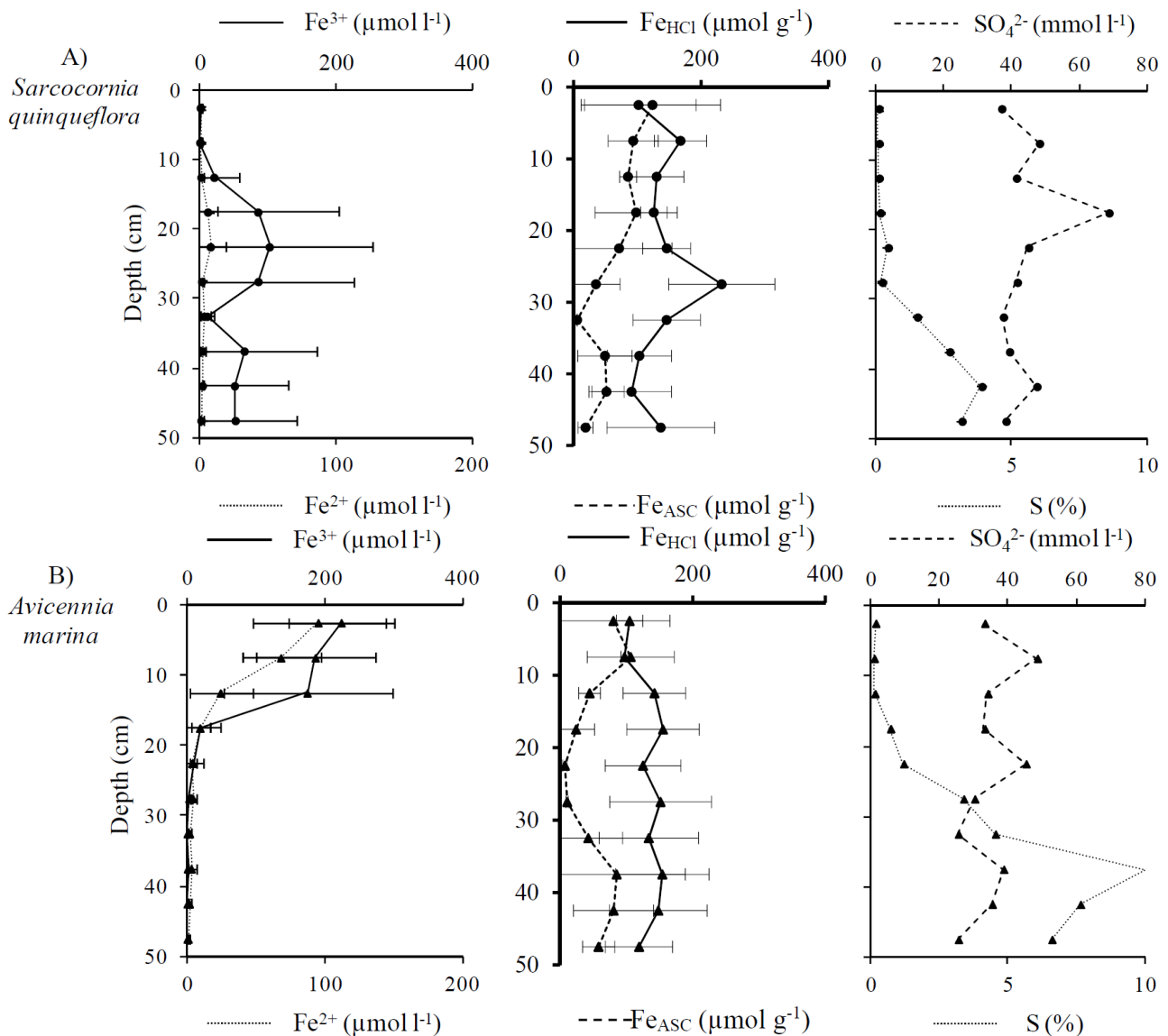


Figure 5. Cont.

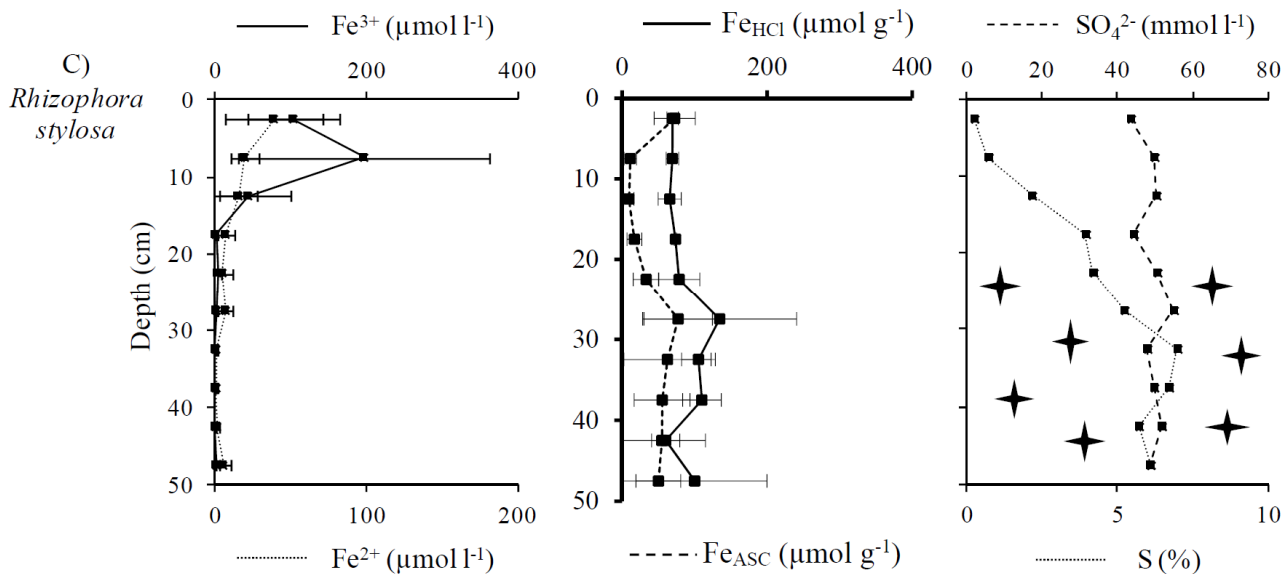


Figure 5. Mean concentrations ($n = 3$) and standard deviation of dissolved iron species (Fe^{2+} and Fe^{3+}), solid iron phases extracted by ascorbate (Fe_{ASC}) and by HCl 1N (Fe_{HCl}). Concentrations ($n = 1$) in SO_4^{2-} and total particulate sulfur (S) in sediments of the three vegetation stands. Depth where total dissolved sulfide was detected is indicated by stars.

3.3. Distribution and Speciation of Limited Key Nutrients: Nitrogen and Phosphorus

Although low N and P availabilities, mangroves are a productive ecosystem [47], mainly as a result of the high recycling capacity of the dissolved pool by vascular plants and micro-organisms [8,48]. N and P limitations may be directly linked to soil elevation and nutrients inputs frequencies by tides or river along the existing zonation [49–51]. Mangrove trees on river banks and on the shoreline can form a strong and dense fringing stand, while mangroves developing at higher elevations usually form dwarf stands [52] as it is the case in New Caledonia.

3.3.1. Distribution and Speciation of Nitrogen Species along the Mangrove Zonation

In the three vegetation stands, DON presented the highest concentrations of the whole dissolved nitrogen species, ranging from 20 to 165 $\mu\text{mol}\cdot\text{L}^{-1}$ (Figure 6). Despite the differences in productivity and organic accumulation in the sediment between the 3 stands, DON concentrations in their soils were not statistically different. Our study demonstrates that from the land-side to the sea-side of the mangrove, at least in the upper layer, the sediment was characterized by increases in water content, salinity and TOC (Section 3.1). However, at depth in every stands, the sediment was rich of decaying *Rhizophora* roots from a previous phase of mangrove colonization, resulting in high and homogenous organic content. Alongi *et al.* [53] suggested that the burial and preservation of a dead root stock and little degradation can be a nutrients conservation process in mangrove soils, and this is probably the case in our studied site. We thus suggest that the stock of decaying *Rhizophora* roots may have induced the high measured DON concentrations, up to $165.5 \pm 48 \mu\text{mol}\cdot\text{L}^{-1}$. The poorest layer in sedimentary organic carbon, *i.e.*, the upper horizon of the salt-flat, was also the poorest in DON. In addition, this horizon was characterized by the highest redox conditions, as a result of the low organic enrichment and longer

dry-period, which can favor ammonification and nitrification. DON production from decomposing organic matter may promote bacterial ammonification processes [54]. In fact, in the salt-flat stand, NH_4^+ accumulates at depth within the organic-rich and anoxic sediments ($31.0 \pm 2.1 \mu\text{mol}\cdot\text{L}^{-1}$ at 50 cm depth, Figure 6). This large amount may result (i) from its production linked to the high organic matter content; (ii) and/or from the absence of a root system that can uptake it; (iii) and/or eventually from possible dissimilatory nitrate reduction to ammonium (DNRA) processes. In some mangroves of New Caledonia, DNRA can account for 10%–60% of total nitrate reduction [55], and favors nitrogen retention, which otherwise would have been denitrified to ammonium. In addition, organic enrichment and production of dissolved sulfides favor DNRA by inhibiting denitrification. In the upper oxic zones, the absence of NH_4^+ may reflect nitrification processes [56]. NO_x concentrations were the highest in this layer reaching $4 \mu\text{mol}\cdot\text{L}^{-1}$ (Figure 6). In addition, crab burrows, by increasing the surface area of sediment available for diffusive oxygen exchanges, are privileged sites for nitrification [39,57,58]. Within the vegetated stand, *i.e.*, *Avicennia* and *Rhizophora*, NH_4^+ and NO_x concentrations in pore-waters were very low at all depths (Figure 5), probably because they were subject to plant uptake as soon as they were produced. Clough [59] and Alongi [48] showed that 90% of the NH_4^+ mangrove consumption is carried through the root system. Vegetated zones are zones of consumption of DIN, which is facilitated by the rapid turnover between producers and consumption.

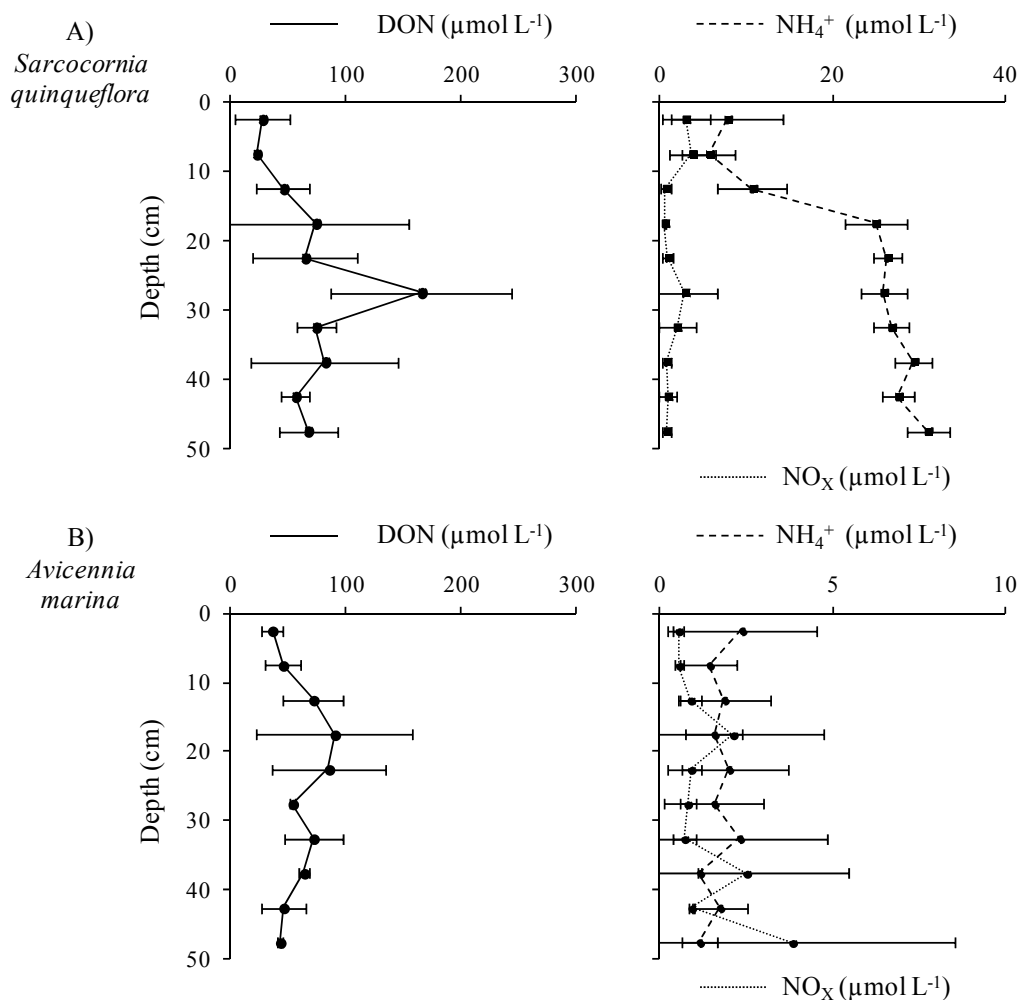


Figure 6. Cont.

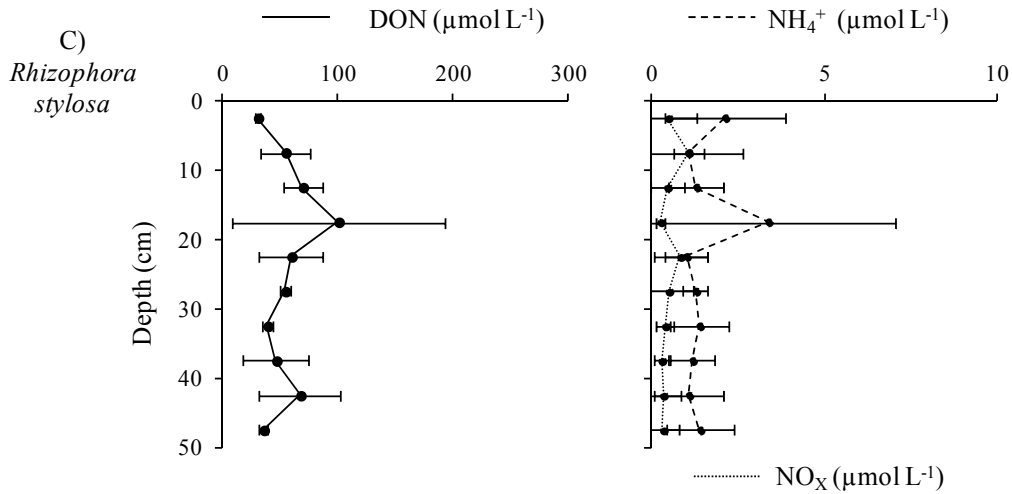


Figure 6. Mean concentrations ($n = 3$) and standard deviation of dissolved organic nitrogen (DON), nitrate + nitrite (NO_x) and NH_4^+ in sediments of the three vegetation stands. Please note differences in y-axis scales for the NH_4^+ and NO_x between the three vegetation stands.

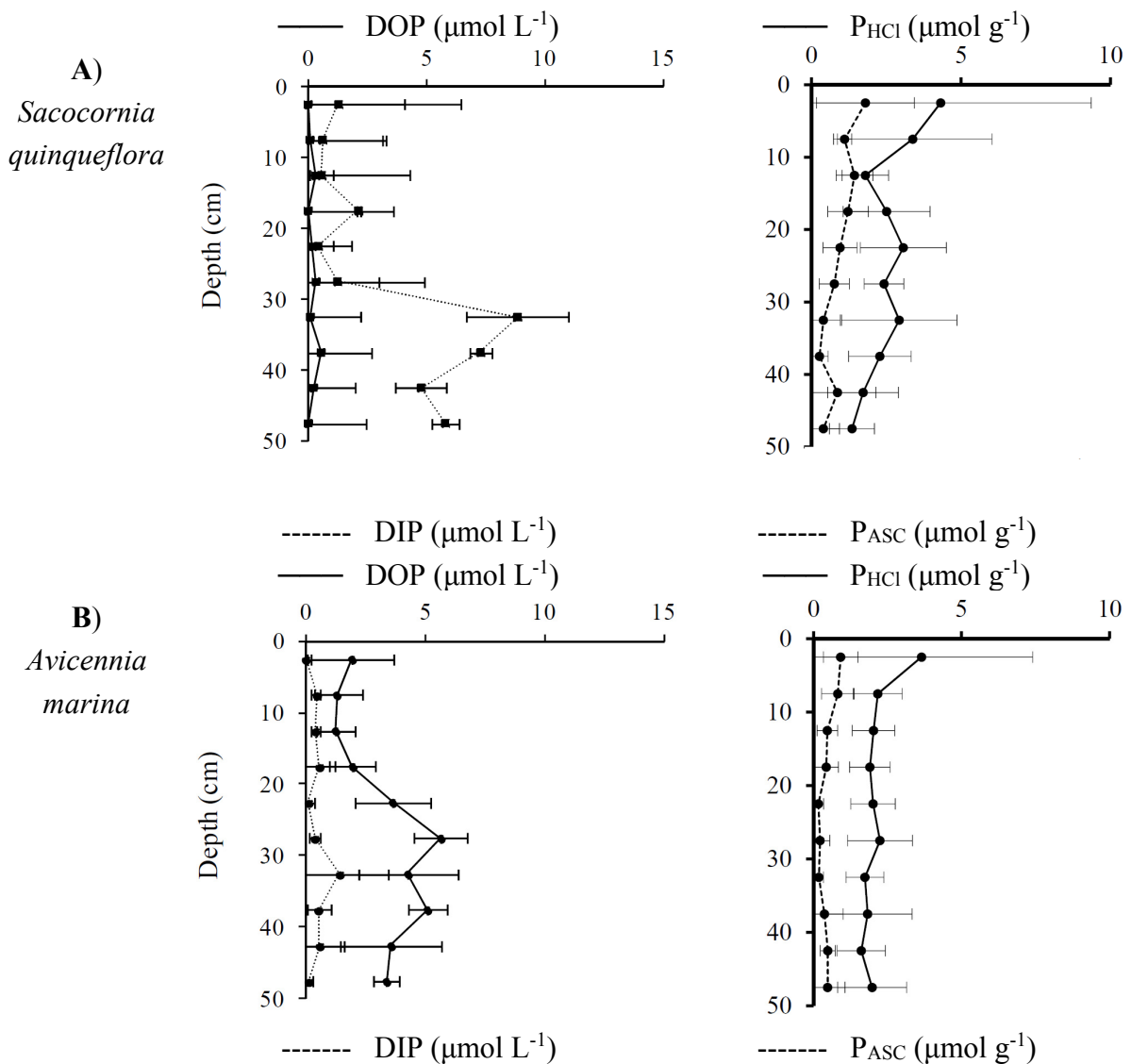


Figure 7. Cont.

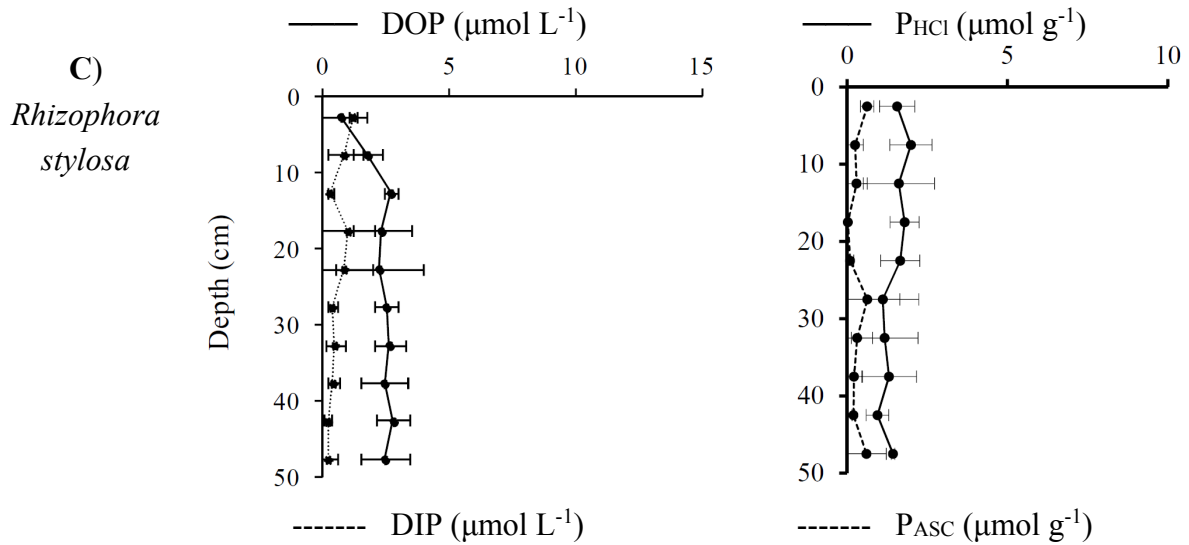


Figure 7. Mean concentrations ($n = 3$) and standard deviation of dissolved organic and inorganic phosphorus (DOP and DIP), and solid phosphorus phases extracted by ascorbate (P_{ASC}) and by HCl 1N (P_{HCl}) in sediments of the three vegetation stands.

3.3.2. Distribution and Speciation of Phosphorus Species along the Mangrove Zonation

The solid fractions of phosphorus (P_{ASC} and P_{HCl}) decreased from the land-side to the sea-side of the mangrove (Figure 7). In addition, concentrations decreased with depth, for instance within the salt-flat, P_{ASC} decreased from $1.8 \pm 1.6 \mu\text{mol} \cdot \text{g}^{-1}$ to less than $0.5 \mu\text{mol} \cdot \text{g}^{-1}$, and P_{HCl} from $4.3 \pm 3.7 \mu\text{mol} \cdot \text{g}^{-1}$ to less than $1.5 \mu\text{mol} \cdot \text{g}^{-1}$ (Figure 7a). Indeed, iron oxides constitute an enormous trap of inorganic phosphorus in oxic sediment zones, but their dissolution result in quick DIP release in pore-waters. Consequently, we suggest that the decrease of total solid fractions of phosphorus can result from the iron oxide dissolution evidenced earlier. In addition, the total phosphorus decreased from land-side to sea-side, probably also resulted from the process of iron loss due to the gradient of oxidation-reduction processes coupled to increased plant uptake. Dissolved phosphorus concentrations in pore-waters depends both on biological activity (root exudation, bacterial decomposition and uptake by root systems, [60]) and on abiotic factors as adsorption and desorption on iron hydroxides and oxyhydroxides [32,33,61]. DOP concentrations were very low beneath each mangrove stand, but increased with depth beneath *Avicennia* and *Rhizophora*, up to 5 and $3.0 \mu\text{mol} \cdot \text{L}^{-1}$, respectively, probably as a result of root system development and an increase of root exudates. In pore-waters, the presence of DOP is supplied by root-system exudates and sedimentary OM decomposition (Figure 7). In the upper layer of the salt-flat, the poorly developed root system of *Sarcocornia* and the low organic accumulation leads to low DOP concentrations ($<1 \mu\text{mol} \cdot \text{L}^{-1}$, Figure 7). In parallel, DOP decomposition by bacteria should lead to an increase in DIP concentrations. However, DIP concentrations were low except in the salt-flat, where they increased below 30 cm depth (Figure 7a). In the anoxic zone of salt-flat, where the uptake by plants is negligible, DIP concentrations increased with depth, up to $8 \mu\text{mol} \cdot \text{L}^{-1}$, and the dissolved Fe/P ratio remained low (Table 2). However, according to high values of particulate Fe/P ratios calculated in this zone, P already appears as a limiting nutrient comparatively to marine sediment where a Fe/P ratio about 10 ± 4 is evaluated [33,62]. In the vegetated mangroves, DIP concentrations remained always very low and the

ratios Fe/P in dissolved phase exceeded 44 in upper sediments colonized by root systems (Table 2). Moreover, Fe/P ratios in reactive particulate fraction are twofold higher than those calculated in the salt-flat, highlighting a strong deficit of adsorbed P onto iron oxides in mangrove stands. This result may evidences that in *Avicennia* and *Rhizophora* stands, as soon as DIP is released from iron oxide reduction, there is a fast assimilation by the roots system, which does not exist in the salt-flat area. This process may explain low DIP concentrations in pore-water of the vegetated zone and its accumulation in the salt-flat.

Table 2. Mean Fe/P ratios in upper sediments (0–15 cm) and underlying sediments (15–50 cm) of the three mangrove vegetation stands. *This vertical limit at 15 cm was chosen as a function of TOC content and redox conditions. The upper layer reflecting a more active layer.*

Ratio	Fraction	Depth (cm)	Salt Flat	<i>Avicennia</i> Stand	<i>Rhizophora</i> Stand
Fe/P	Dissolved inorganic fraction	0–15	4	94	44
		15–50	9	20	19
	Particulate reactive fraction (Ascorbate)	0–15	73	121	70
		15–50	79	147	191
	Particulate amorphous fraction (HCl)	0–15	78	79	50
		15–50	71	77	70

4. Conclusions

Mangrove zonation, resulting from differences in soil elevation and thus differences in nutrient inputs and soil salinity, leads to specific distribution and speciation of the studied elements, and may regulate the ability of a mangrove ecosystem to be a source or a sink of these compounds. In upstream area, the sediment is frequently emerged, leading to a high rate of evaporation and thus, in high salinities and low pore-water content. In these conditions, only dwarfs’ stands develop, which lead to a low organic carbon accumulation in sediment. However, TOC content as well as the contribution of mangrove debris to the organic pool increased towards the sea-side of the mangrove. These increases in TOC and water content led to decreasing redox values towards the sea-side. There were no clear gradients of dissolved inorganic nutrients along the zonation. However, their accumulation in a deep, anoxic, and organic rich layer in the salt-flat evidences their production from the sedimentary organic stock. While their absence in the vegetated zone may result from their rapid uptake by mangrove trees as soon as they are produced. In the three vegetation stands, there is a significant increase in total particulate sulfur below the upper suboxic zone, evidencing iron oxide reduction as well as sulfate-reduction processes. In addition to reduction processes, intense re-oxidation of aqueous Fe(II) and Fe-sulfides are suspected, leading to the high dissolved iron concentrations as well as low pH. The latter decreased from the land-side to the sea-side as a result on the one hand on the increasing amount of organic matter to be decomposed and, on the other hand on possible sulfide oxidation, due to frequent tidal inundation of *Rhizophora* stand. Tidal fluctuations may be a major cause for continuous Fe reduction-oxidation cycles, which may be thus more intense when the stand is closer to the shore. Additionally, concentrations of solid phase Fe decreased from the land-side to the sea-side of the mangrove, confirming the hypothesis of a loss of Fe from the salt-flat to the *Rhizophora*. These increased oxidation-reduction processes from the land to the

sea may also explain the fact that total phosphorus, of which cycling is strongly linked to iron oxides cycle, decreased along a land-sea gradient in the mangrove. Within a future research effort, concentrations and speciation of Fe and P in the dissolved and in the particulate phases in a mangrove tidal creek will be determined as a function of tides to confirm our hypothesis of elements loss towards the coastal area as a result of frequent re-oxidation due to tidal cycles.

Acknowledgments

The authors gratefully acknowledge the staff of the Saint Vincent shrimp farm, Christophe Canel, and of the IFREMER station for their valuable help and the access to their laboratory. We thank Audrey Leopold for her assistance with field and laboratory works, and Philippe Gerard (Laboratoire de Chimie Marine) from IRD-Nouméa for the chemical analysis. This work was supported by the ZONECO Program, the Northern Province and Southern Province of New Caledonia. The authors are grateful to two anonymous reviewers who critically evaluated this manuscript and provided many useful suggestions that have helped to improve its quality.

Author Contributions

N.M., L.D.P., C.M. and J.D. performed the field work. N.M. and J.D. performed the chemical analyses. J.D., C.M., and T.M. wrote the manuscript. All authors discussed the results and contributed to the manuscript.

Conflicts of Interest

The authors declare no conflict of interest.

References

1. Giri, C.; Ochieng, E.; Tieszen, L.L.; Zhu, Z.; Singh, A.; Loveland, T.; Masek, J.; Duke, N. Status and distribution of mangrove forests of the world using earth observation satellite data. *Glob. Ecol. Biogeogr.* **2011**, *20*, 154–159.
2. Duke, N.C.; Meynecke, J.-O.; Dittmann, S.; Ellison, A.M.; Anger, K.; Berger, U.; Cannicci, S.; Diele, K.; Ewel, K.C.; Field, C.D.; *et al.* A world without mangroves? *Science* **2007**, *317*, 41–42.
3. Barbier, E.B. Valuing ecosystem services as productive inputs. *Econ. Policy* **2007**, *22*, 177–229.
4. Walters, B.B. Mangrove forests and environmental security. In *Forests in the Balance: Linking Tradition and Technology, XXII IUFRO World Congress*; Innes, J.I., Edwards, I.K, Wilford, D.J., Eds.; International Forestry Review: Brisbane, Australia, 2006; Volume 7, p. 290.
5. Chmura, G.L.; Anisfeld, S.C.; Cahoon, D.R.; Lynch, J.C. Global carbon sequestration in tidal, saline wetland soils. *Glob. Biogeochem. Cycles* **2003**, *17*, 1111.
6. Donato, D.C.; Kauffman, J.B.; Murdiyarso, D.; Kurnianto, S.; Stidham, M.; Kanninen, M. Mangrove among the most carbon-rich forests in the tropics. *Nat. Geosci.* **2011**, *4*, 293–297.
7. Kristensen, E.; Bouillon, S.; Dittmar, T.; Marchand, C. Organic carbon dynamics in mangrove ecosystems: A review. *Aquat. Bot.* **2008**, *89*, 201–219.

8. Alongi, D.M.; Clough, B.F.; Robertson, A.I. Nutrient-use efficiency in arid-zone forests of the mangroves *rhizophora stylosa* and *avicennia marina*. *Aquat. Bot.* **2005**, *82*, 121–131.
9. Alongi, D.M.; Tirendi, F.; Clough, B.F. Below-ground decomposition of organic matter in forests of the mangrove *rhizophora stylosa* and *avicennia marina* along the arid coast of western australia. *Aquat. Bot.* **2000**, *68*, 97–122.
10. Marchand, C.; Baltzer, F.; Lallier-Vergès, E.; Albéric, P. Pore-water chemistry in mangrove sediments: Relationship with species composition and developmental stages (French Guiana). *Mar. Geol.* **2004**, *208*, 361–381.
11. Ferreira, T.O.; Otero, X.L.; Vidal-Torrado, P.; Macías, F. Effects of bioturbation by root and crab activity on iron and sulfur biogeochemistry in mangrove substrate. *Geoderma* **2007**, *142*, 36–46.
12. McKee, K.L. Soil physicochemical patterns and mangrove species distribution—Reciprocal effects? *J. Ecol.* **1993**, *81*, 477–487.
13. Walsh, G.E. Mangroves: A review. In *Ecology of Halophytes*; Queen, R.J.R.H., Ed.; Academic Press: Waltham, MA, USA, 1974; pp. 51–174.
14. Ellison, J.C. Impacts of sediment burial on mangroves. *Mar. Pollut. Bull.* **1999**, *37*, 420–426.
15. Clark, M.W.; McConchie, D.; Lewis, D.W.; Saenger, P. Redox stratification and heavy metal partitioning in *avicennia*-dominated mangrove sediments: A geochemical model. *Chem. Geol.* **1998**, *149*, 147–171.
16. Virly, S. Atlas des mangroves de nouvelle-calédonie. In *Typologies et Biodiversité des Mangroves de Nouvelle-Calédonie*; ZoNéCo: Nouméa, New Caledonia, 2006; p. 213.
17. Marchand, C.; Allenbach, M.; Lallier-Vergès, E. Relationships between heavy metals distribution and organic matter cycling in mangrove sediments (conception bay, New Caledonia). *Geoderma* **2011**, *160*, 444–456.
18. Marchand, C.; Fernandez, J.M.; Moreton, B.; Landi, L.; Lallier-Vergès, E.; Baltzer, F. The partitioning of transitional metals (Fe, Mn, Ni, Cr) in mangrove sediments downstream of a ferrallitized ultramafic watershed (New Caledonia). *Chem. Geol.* **2012**, *300–301*, 70–80.
19. Baltzer, F. Géodynamique de la sédimentation et diagenèse précoce en domaine ultrabasique—Nouvelle calédonie. *Trav. Doc. ORSTOM* **1982**, *152*, 283.
20. Song, J.; Luo, Y.M.; Zhao, Q.G.; Christie, P. Novel use of soil moisture samplers for studies on anaerobic ammonium fluxes across lake sediment-water interfaces. *Chemosphere* **2003**, *50*, 711–715.
21. Marchand, C.; Lallier-Vergès, E.; Baltzer, F.; Albéric, P.; Cossa, D.; Baillif, P. Heavy metals distribution in mangrove sediments along the mobile coastline of French Guiana. *Mar. Chem.* **2006**, *98*, 1–17.
22. Vismann, B. Sulphide exposure experiments: The sulphide electrode and a set-up automatically controlling sulphide, oxygen and pH. *J. Exp. Mar. Biol. Ecol.* **1996**, *204*, 131–140.
23. Stookey, L.L. Ferrozine—A new spectrophotometric reagent for iron. *Anal. Chim. Acta* **1970**, *42*, 779–781.
24. Strickland, J.D.H.; Parsons, T.R. *A Practical Handbook of Seawater Analysis*; Fisheries Research Board of Canada: Ottawa, Ontario, Canada, 1972; Volume 197.
25. Rodier, J. L'analyse de L'eau, Eaux Naturelles, Eaux Résiduares, Eau de Mer; Dunod: Paris, France, 1976; p. 364.

26. Holmes, R.M.; Aminot, A.; K erouel, R.; Hooker, B.A.; Peterson, B.J. A simple and precise method for measuring ammonium in marine and freshwater ecosystems. *Can. J. Fish. Aquat. Sci.* **1999**, *56*, 1801–1808.
27. Bendschneider, K.; Robinson, R.J. A new spectrophotometric method for the determination of nitrite in sea water. *J. Mar. Res.* **1952**, *11*, 87–96.
28. Murphy, J.; Riley, J.P. A modified single solution method for determination of phosphate in natural waters. *Anal. Chim. Acta* **1962**, *26*, 31–36.
29. Raimbault, P.; Pouvesle, W.; Diaz, F.; Garcia, N.; Semp er e, R. Wet-oxidation and automated colorimetry for simultaneous determination of organic carbon, nitrogen and phosphorus dissolved in seawater. *Mar. Chem.* **1999**, *66*, 161–169.
30. Marchand, C.; Lallier-Verg es, E.; Disnar, J.R.; K eravis, D. Organic carbon sources and transformations in mangrove sediments: A rock-eval pyrolysis approach. *Org. Geochem.* **2008**, *39*, 408–421.
31. Lafargue, E.; Marquis, F.; Pillot, D. Rock-eval 6 applications in hydrocarbon exploration, production and soil contamination studies. *Rev. Inst. Fr. P et.* **1998**, *53*, 421–437.
32. Deborde, J.; Anschutz, P.; Chaillou, G.; Etcheber, H.; Commarieu, M.V.; Lecroart, P.; Abril, G. The dynamics of phosphorus in turbid estuarine systems: Example of the Gironde estuary (France). *Limnol. Oceanogr.* **2007**, *52*, 862–872.
33. Anschutz, P.; Zhong, S.; Sundby, B.; Mucci, A.; Gobeil, C. Burial efficiency of phosphorus and the geochemistry of iron in continental margin sediments. *Limnol. Oceanogr.* **1998**, *43*, 53–64.
34. Kostka, J.E.; Luther III, G.W. Partitioning and speciation of solid phase iron in saltmarsh sediments. *Geochim. Cosmochim. Acta* **1994**, *58*, 1701–1710.
35. Anschutz, P.; Chaillou, G.; Lecroart, P. Phosphorus diagenesis in sediment of the Thau lagoon. *Estuar. Coast. Shelf Sci.* **2007**, *72*, 447–456.
36. Bouillon, S.; Dahdouh-Guebas, F.; Rao, A.V.V.S.; Koedam, N.; Dehairs, F. Sources of organic carbon in mangrove sediments: Variability and possible ecological implications. *Hydrobiologia* **2003**, *495*, 33–39.
37. Marchand, C.; Disnar, J.R.; Lallier-Verg es, E.; Lottier, N. Early diagenesis of carbohydrates and lignin in mangrove sediments subject to variable redox conditions (French Guiana). *Geochim. Cosmochim. Acta* **2005**, *69*, 131–142.
38. Lallier-Verg es, E.; Marchand, C.; Disnar, J.R.; Lottier, N. Origin and diagenesis of lignin and carbohydrates in mangrove sediments of Guadeloupe (French West Indies): Evidence for a two-step evolution of organic deposits. *Chem. Geol.* **2008**, *255*, 388–398.
39. Botto, F.; Iribarne, O. Contrasting effects of two burrowing crabs (*Chasmagnathus granulata* and *Uca uruguayensis*) on sediment composition and transport in estuarine environments. *Estuar. Coast. Shelf Sci.* **2000**, *51*, 141–151.
40. Nielsen, T.; Andersen, F. . Phosphorus dynamics during decomposition of mangrove (*Rhizophora apiculata*) leaves in sediments. *J. Exp. Mar. Biol. Ecol.* **2003**, *293*, 73–88.
41. Thibodeau, F.R.; Nickerson, N.H. Differential oxidation of mangrove substrate by *Avicennia germinans* and *Rhizophora mangle*. *Am. J. Bot.* **1986**, *73*, 512–516.

42. Dublet, G.; Juillot, F.; Morin, G.; Fritsch, E.; Fandeur, D.; Ona-Nguema, G.; Brown, G.E., Jr. Ni speciation in a new caledonian lateritic regolith: A quantitative x-ray absorption spectroscopy investigation. *Geochim. Cosmochim. Acta* **2012**, *95*, 119–133.
43. Fernandez, J.-M.; Ouillon, S.; Chevillon, C.; Douillet, P.; Fichez, R.; Gendre, R.L. A combined modelling and geochemical study of the fate of terrigenous inputs from mixed natural and mining sources in a coral reef lagoon (New Caledonia). *Mar. Pollut. Bull.* **2006**, *52*, 320–331.
44. Noël, V.; Marchand, C.; Juillot, F.; Ona-Nguema, G.; Viollier, E.; Marakovic, G.; Olivi, L.; Delbes, L.; Gelebart, F.; Morin, G. Exafs analysis of iron cycling in mangrove sediments downstream a lateritized ultramafic watershed (Vavouto Bay, New Caledonia). *Geochim. Cosmochim. Acta* **2014**, *136*, 211–228.
45. Canfield, D.E.; Raiswell, R.; Bottrell, S.H. The reactivity of sedimentary iron minerals toward sulfide. *Am. J. Sci.* **1992**, *292*, 659–683.
46. Holmer, M.; Kristensen, E.; Banta, G.; Hansen, K.; Jensen, M.H.; Bussawarit, N. Biogeochemical cycling of sulfur and iron in sediments of a south-east asian mangrove, phuket island, thailand. *Bioelectrochemistry* **1994**, *26*, 145–161.
47. Bouillon, S.; Borges, A.V.; Castañeda-Moya, E.; Diele, K.; Dittmar, T.; Duke, N.C.; Kristensen, E.; Lee, S.Y.; Marchand, C.; Middelburg, J.J.; *et al.* Mangrove production and carbon sinks: A revision of global budget estimates. *Glob. Biogeochem. Cycles* **2008**, *22*, GB2013.
48. Alongi, D.M. The dynamics of benthic nutrient pools and fluxes in tropical mangrove forests. *J. Mar. Res.* **1996**, *54*, 123–148.
49. Feller, I.C.; Lovelock, C.; McKee, K.L. Nutrient addition differentially affects ecological processes of *avicennia germinans* in nitrogen *versus* phosphorus limited mangrove ecosystems. *Ecosystems* **2007**, *10*, 347–359.
50. Feller, I.C. Effects of nutrient enrichment on growth and herbivory of dwarf red mangrove (*Rhizophora mangle*). *Ecol. Monogr.* **1995**, *65*, 477–505.
51. Lovelock, C.E.; Feller, I.C.; McKee, K.L.; Engelbrecht, B.M.J.; MC., B. The effect of nutrient enrichment on growth, photosynthesis and hydraulic conductance of dwarf mangroves in Panama. *Funct. Ecol.* **2004**, *18*, 25–33.
52. Dangremond, E.M.; Feller, I.C. Functional traits and nutrient limitation in the rare mangrove *pelliciera rhizophorae*. *Aquat. Bot.* **2014**, *116*, 1–7.
53. Alongi, D.M.; Trott, L.A.; Wattayakorn, G.; Clough, B.F. Below ground nitrogen cycling in relation to net canopy production in mangrove forests of Southern Thailand. *Mar. Biol.* **2002**, *140*, 855–864.
54. Badr, E.-S.A.; Tappin, A.D.; Achterberg, E.P. Distributions and seasonal variability of dissolved organic nitrogen in two estuaries in sw england. *Mar. Chem.* **2008**, *110*, 153–164.
55. Molnar, N.; Welsh, D.T.; Marchand, C.; Deborde, J.; Meziane, T. Impacts of shrimp farm effluent on water quality, benthic metabolism and n-dynamics in a mangrove forest (New Caledonia). *Estuar. Coast. Shelf Sci.* **2013**, *117*, 12–21.
56. Canfield, D. Organic matter oxidation in marine sediments. In *Interactions of C, N, P and S Biogeochemical Cycles and Global Change*; Wollast, R.; Mackenzie, F.; Chou, L., Eds.; Springer Berlin Heidelberg: Berlin, Germany, 1993; Volume 4, pp. 333–363.

57. Kristensen, E.; Alongi, D.M. Control by fiddler crabs (*Uca vocans*) and plant roots (*Avicennia marina*) on carbon, iron, and sulfur biogeochemistry in mangrove sediment. *Limnol. Oceanogr.* **2006**, *51*, 1557–1571.
58. Jordan, M.A.; Welsh, D.T.; Dunn, R.J.K.; Teasdale, P.R. Influence of *trypaea australiensis* population density on benthic metabolism and nitrogen dynamics in sandy estuarine sediment: A mesocosm simulation. *J. Sea Res.* **2009**, *61*, 144–152.
59. Clough, B.F. Primary productivity and growth of mangrove forests. In *Tropical Mangrove Ecosystems*; Robertson, A.I., Alongi, D.M., Eds.; American Geophysical Union: Washington, DC, USA, 1992; Volume Coastal and Estuarine Study No.41, pp. 225–250.
60. Gleason, S.M.; Ewel, K.C.; Hue, N. Soil redox conditions and plant–soil relationships in a micronesian mangrove forest. *Estuar. Coast. Shelf Sci.* **2003**, *56*, 1065–1074.
61. Jensen, H.S.; Mortensen, P.B.; Andersen, F.Ø.; Rasmussen, E. Phosphorus cycling in coastal marine sediment, Aarhus Bay, Denmark. *Mar. Ecol. Prog. Ser.* **1995**, *293*, 49–58.
62. Cha, H.J.; Lee, C.B.; Kim, B.S.; Choi, M.S.; Ruttenberg, K.C. Early diagenetic redistribution and burial of phosphorus in the sediments of the southwestern East Sea (Japan Sea). *Mar. Geol.* **2005**, *216*, 127–143.

© 2015 by the authors; licensee MDPI, Basel, Switzerland. This article is an open access article distributed under the terms and conditions of the Creative Commons Attribution license (<http://creativecommons.org/licenses/by/4.0/>).